Two appendages homologous between basal bodies and centrioles are formed using distinct *Odf2* domains

Kazuhiro Tateishi,[1] Yuji Yamazaki,[1] Tomoki Nishida,[2] Shin Watanabe,[1] Koshi Kunimoto,[3] Hiroaki Ishikawa,[4] and Sachiko Tsukita[1]

[1]Laboratory of Biological Science, Graduate School of Frontier Biosciences and Graduate School of Medicine, Osaka University, Osaka 565-0871, Japan
[2]Research Center for Ultra-high Voltage Electron Microscopy, Osaka University, Osaka 567-0047, Japan
[3]Department of Pathology, Stanford University School of Medicine, Stanford, CA 94305
[4]Department of Biochemistry and Biophysics, University of California, San Francisco, San Francisco, CA 94158

Ciliogenesis is regulated by context-dependent cellular cues, including some transduced through appendage-like structures on ciliary basal bodies called transition fibers and basal feet. However, the molecular basis for this regulation is not fully understood. The *Odf2* gene product, ODF2/cenexin, is essential for both ciliogenesis and the formation of the distal and subdistal appendages on centrioles, which become basal bodies. We examined the effects of *Odf2* deletion constructs on ciliogenesis in *Odf2*-knockout F9 cells. Electron microscopy revealed that ciliogenesis and transition fiber formation required the ODF2/cenexin fragment containing amino acids (aa) 188–806, whereas basal foot formation required aa 1–59 and 188–806. These sequences also formed distal and subdistal appendages, respectively, indicating that the centriole appendages are molecularly analogous to those on basal bodies. We used the differential formation of appendages by *Odf2* deletion constructs to study the incorporation and function of molecules associated with each appendage type. We found that transition fibers and distal appendages were required for ciliogenesis and subdistal appendages stabilized the centrosomal microtubules.

Introduction

Both ciliary basal bodies and centrioles display two kinds of appendage-like structures: transition fibers (TFs) and basal feet (BF) in ciliary basal bodies, and distal and subdistal appendages (DAs and SAs) in centrioles (Gibbons, 1961; Anderson, 1972; Vorobjev and Chentsov, 1982; Bornens et al., 1987; Paintrand et al., 1992). The presence of these appendages depends on the product of the *Odf2* gene, ODF2/cenexin. This protein was first identified as a specific component of the sperm-tail outer dense fiber, and later as a ubiquitous component of centrioles, in which it is localized to the DAs and SAs (Oko and Clermont, 1988; Lange and Gull, 1995; Brohmann et al., 1997; Nakagawa et al., 2001; Ishikawa et al., 2005; Kunimoto et al., 2012). The targeted recombination of *Odf2* in F9 cells showed that the *Odf2* gene has essential roles in ciliogenesis and in forming the DAs and SAs of centrioles, which become basal bodies.

Among other characterized centrosome proteins, CEP164, CCDC123/CEP89/CEP123, CCDC41, SCLT1, and FBF1 were identified as DA components (Graser et al., 2007; Sillibourne et al., 2011; Tanos et al., 2013). In contrast, ninein, centriolin, ε-tubulin, and CEP170 are associated with SAs, suggesting that the two types of appendages have different roles (Bouckson-Castaing et al., 1996; Mogensen et al., 2000; Chang et al., 2003; Gromley et al., 2003; Guarguaglini et al., 2005). At least some of these components associate with ODF2/cenexin to form *Odf2*-based multifunctional molecular platforms in the centriole appendages, including platforms for Rab8 and Rab11, which are associated with DAs and SAs (Gromley et al., 2005; Graser et al., 2007; Ibi et al., 2011; Hehnly et al., 2012; Schmidt et al., 2012; Tanos et al., 2013).

The *Odf2* gene expression can be completely suppressed by deleting exons 6–9 (Ex-6–Ex-9), and this deletion in F9 cells

K. Tateishi and Y. Yamazaki contributed equally to this paper.

Correspondence to Sachiko Tsukita: atsukita@biosci.med.osaka-u.ac.jp

Abbreviations used in this paper: BF, basal feet; DA, distal appendage; MTOC, microtubule-organizing center; SA, subdistal appendage; TF, transition fiber; UHVEMT, ultra-high voltage electron microscopic tomography.

The Rockefeller University Press $30.00
J. Cell Biol. Vol. 203 No. 3 417–425
www.jcb.org/cgi/doi/10.1083/jcb.201303071

completely abrogates ciliogenesis. However, a recent report showed that the deletion of *Odf2* Ex-6 and Ex-7 in mice permits the generation of cilia, due to the expression of *Odf2's* C-terminal domains, but the BF of the ciliary basal bodies are lost (Kunimoto et al., 2012). Furthermore, in the trachea of these BF-lacking *Odf2* mutant mice, the normally regular apical microtubule networks show aberrant organization. These findings shed light on the role of BF, especially in planar cell polarity (PCP) and the arrangement of apical microtubules. In addition, because centriolin is a component of BF, and the centriolin-based Rab11 pathway functions in vesicular trafficking, the BF are thought to play roles in a variety of biological processes (Ullrich et al., 1996; Ren et al., 1998; Knödler et al., 2010; Westlake et al., 2011; Hehnly et al., 2012).

In this study, we used deletion constructs of *Odf2* lacking Ex-6 and Ex-7 (Δ6/7) or Ex-4 and Ex-5 (Δ4/5), as well as a deletion series of *Odf2*'s N-terminal and C-terminal domains, and examined ciliogenesis and the reconstitution of TFs and/or BF of basal bodies, as well as DAs and SAs of centrioles, in an *Odf2*-KO F9 cell line (Ishikawa et al., 2005). The appendage-modified cells enabled us to identify the *Odf2* sequences responsible for ciliogenesis and for reconstituting each of the appendages.

Results and discussion

The N terminus of *Odf2* is dispensable for ciliogenesis

We first transfected full-length GFP-tagged *Odf2* into *Odf2*-KO F9 cells, and immunostained for GFP (to detect GFP-ODF2/cenexin), acetylated α-tubulin (to detect primary cilia), and γ-tubulin (to detect basal bodies and centrioles; Fig. 1, A and B). The full-length *Odf2* gene product was recruited to centrioles and ciliary basal bodies, and ciliogenesis was restored in *Odf2*-KO F9 cells by the full-length GFP-tagged *Odf2* construct (Fig. 1, B and C).

Next, to reveal which *Odf2* gene sequences are required for ciliogenesis, we exogenously expressed GFP-tagged *Odf2* deletion constructs in the *Odf2*-KO cells, and examined the immunofluorescent signals for GFP, γ-tubulin, and acetylated α-tubulin (Fig. 1, A and B). The set of *Odf2* deletion constructs was based on the previous finding that the C-terminal regions of ODF2/cenexin are critical for ciliogenesis (Kunimoto et al., 2012). When we examined *Odf2* constructs that lacked certain N-terminal regions, the cells expressing the Ca construct (aa 188–806), but not the Cb (324–806), Cc (459–806), or Cd (613–806) construct, formed stable primary cilia (Fig. 1, A–C). The frequency of primary cilia among *Odf2*-KO F9 cells expressing the Ca construct was comparable to that in cells expressing the full-length construct; in contrast, cilia were quite infrequent in cells expressing Cb, and no cilia were observed in those expressing Cc or Cd. Thus, the N terminus of ODF2/cenexin was dispensable for primary ciliogenesis, and a sequence that was critical for ciliogenesis lay between the Ca and Cb constructs. Consistent with this finding, primary cilia were generated by cells expressing an *Odf2* construct lacking Ex-4 and Ex-5 (Δ4/5) or one lacking Ex-6 and Ex-7 (Δ6/7) without the frame-shift (Fig. 1, B and C). These sequences included the region deleted from the Ca construct.

Furthermore, a nearly full-length construct, containing the two leucine zipper motifs but lacking the C-terminal domain (ΔCd), was not recruited to basal bodies and did not generate primary cilia. The same result was obtained for the N construct. Thus, the 188–806 aa fragment of ODF2/cenexin, which includes the two leucine motifs and the most C-terminal region, was indispensable for stable ciliogenesis; the N terminus was dispensable for it (Fig. 1, A–C; and Fig. S2). In previous reports on ODF2 knockdown experiments, DAs still formed (Graser et al., 2007; Schmidt et al., 2012; Tanos et al., 2013). We expect that low-level, residual ODF2 was sufficient for DA formation in those reports. In support of this idea, as mentioned above, the low-level expression of ODF2 C-terminal domains in mutant mice allowed DAs (and eventually cilia) to be generated (Kunimoto et al., 2012), which was not the case in *Odf2*-KO cells. Together, these findings support the idea that the C-terminal ODF2 domains are required to form DAs, and even low levels of these domains are sufficient for appendage formation.

Ciliogenic constructs of *Odf2* reconstitute transition fibers

To learn the roles of specific *Odf2* domains in the formation of basal body appendages, we transfected *Odf2* deletion constructs, including the ciliogenic and nonciliogenic ones, into *Odf2*-KO F9 cells, and then examined the TFs and BF by electron microscopy (Fig. 1 D, Fig. S1, and Fig. S3 A). To make sure we examined the entire basal body, we used serial thin-section electron microscopy (EM) and ultra-high voltage electron microscopic tomography (UHVEMT). In cells expressing the ciliogenic constructs, i.e., the wild-type (full-length), Δ4/5, Δ6/7, and Ca constructs, TFs were associated with basal bodies at the base of the cilia, connecting them to the plasma membrane (Fig. 1 D, Fig. 3, Fig. S1, and Videos 1–4). These results indicated that the N terminus of *Odf2* is dispensable for forming the molecular platform required to generate TFs and cilia.

ODF2/cenexin exons 4/5 are required to reconstitute the basal feet in ciliogenic constructs

In the cells of *Odf2* mutant mice that expressed only the C-terminal *Odf2* sequences, the TFs formed, but the BF did not (Kunimoto et al., 2012). We therefore examined BF formation in wild-type F9 cells or in *Odf2*-KO F9 cells transfected with the ciliogenic *Odf2*-deletion constructs (Δ4/5, Δ6/7, and Ca) by serial thin-section EM and UHVEMT. We found that the Δ4/5 and Ca constructs did not form BF, whereas the full-length and Δ6/7 constructs did (Fig. 1 D, Fig. 3, Fig. S1, Fig. S3 A, and Videos 1–4), suggesting that Ex-4/5 was required for the formation of BF on basal bodies. The large C-terminal region in the Ca construct (aa 188–806) was required and sufficient for the formation of TFs and for ciliogenesis. Together, these findings demonstrated the domains of *Odf2* required to form TFs and BF on ciliary basal bodies.

The same respective domains of *Odf2* reconstitute the homologous appendage types in ciliary basal bodies and centrioles

It is generally accepted that centrioles become basal bodies, depending on context-dependent cellular cues (Vorobjev and

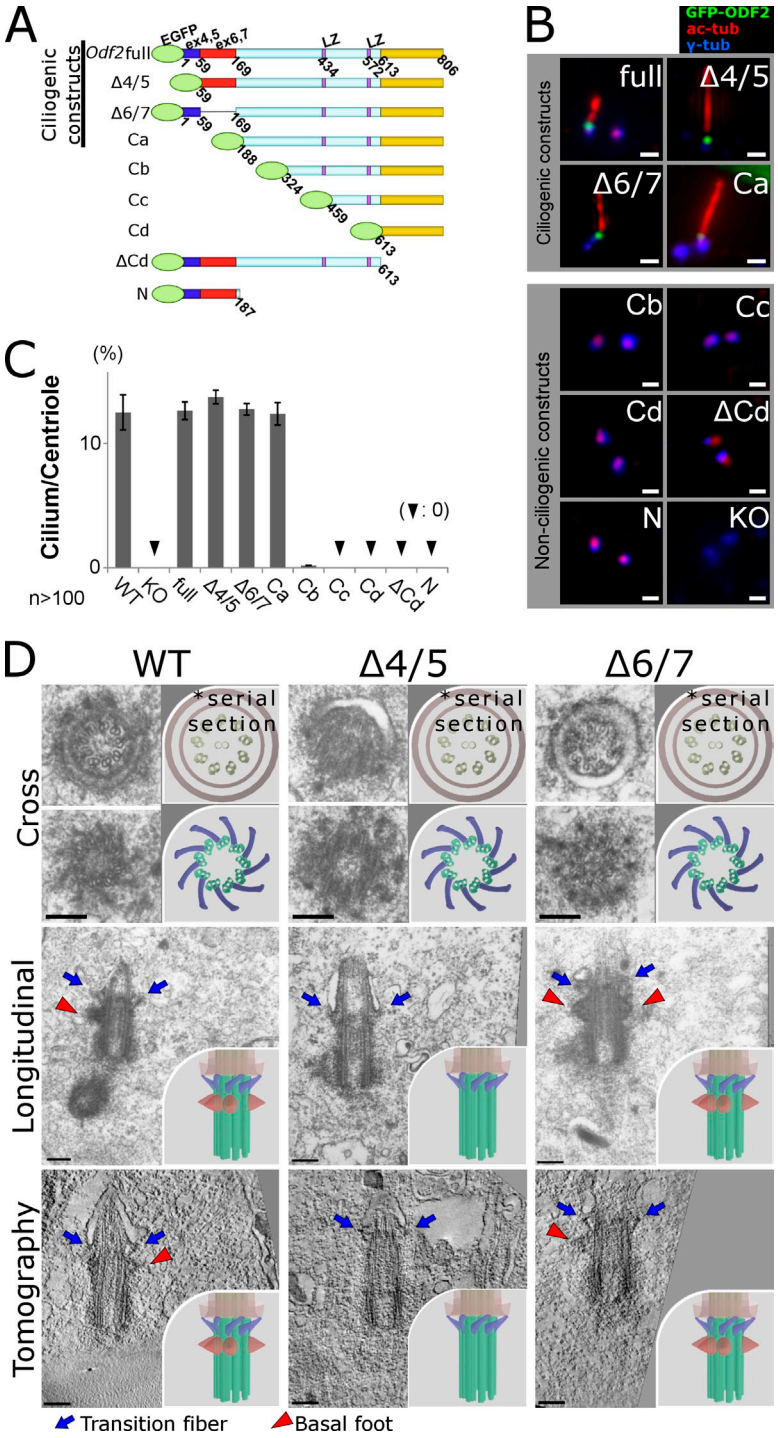

Figure 1. ***Odf2* gene sequences required to generate cilia and reconstitute the appendages of ciliary basal bodies.** (A) Schematic representation of the *Odf2* deletion constructs, which were transfected into *Odf2*-KO F9 cells. LZ, leucine zipper motif. (B) Immunofluorescence for GFP (Odf2), γ-tubulin (centrioles/basal bodies), and acetylated tubulin (primary cilia) to examine the generation of cilia. Bars, 1 µm. (C) Percentage of cilia on centrioles in cells expressing the indicated construct (n > 100 in more than three independent experiments). (D) Electron micrographs showing transition fibers (TFs) and/or basal feet (BF) on ciliary basal bodies. Thin-section electron microscopic images show cross sections (Cross) and longitudinal sections (Longitudinal) of primary cilia. Tomography, UHVEMT images of basal bodies; TFs, blue arrows; BF, red arrowheads; WT, (TF+BF+) basal bodies in WT F9 cells; Δ4/5, (TF+BF−) basal bodies in Δ4/5 construct–expressing *Odf2*-KO F9 cells; Δ6/7, (TF+BF+) basal bodies in Δ6/7 construct–expressing *Odf2*-KO F9 cells. Bars, 0.2 µm. More than five samples were analyzed in each case. The cross section electron micrographs in the top two rows are the same images as in the top two rows of Fig. S3 A, where they are annotated for TFs and BF. Insets, schematic drawings of electron microscopic images of basal bodies.

Chentsov, 1982; Bornens, 2002; Dawe et al., 2007; Hoyer-Fender, 2010; Kobayashi and Dynlacht, 2011; Nigg and Stearns, 2011). The similar morphological characteristics of the appendages for basal bodies and centrosomes was first noted in early EM studies, which identified two kinds of protrusions on the distal sides of the microtubule barrels (Gibbons, 1961; Sorokin, 1962; Anderson, 1972; Dirksen and Satir, 1972; Reed et al., 1984). That is, the TFs of the basal body morphologically resembled the DAs of the centriole, and the BF of the basal body resembled the centriole SAs. Later, the TFs and DAs were found to contain CEP164, CCDC123/CEP89/CEP123, CCDC41, SCLT1, and FBF1 (Graser et al., 2007; Tanos et al., 2013), and the BF and SAs to contain ninein and centriolin (Ishikawa et al., 2005; Vladar and Stearns, 2007; Kunimoto et al., 2012), supporting the structural homology of these appendages. Here we examined this similarity using specific domains of the *Odf2* gene to reconstitute the appendages in ciliary basal bodies and centrioles.

We first examined the centrosomes in cells expressing the *Odf2* ciliogenic constructs that formed TFs, and found that these constructs also formed the centriole DAs. In contrast, the non-ciliogenic constructs did not reconstitute the DAs (Fig. 2, Fig. 3, Fig. S1, Fig. S3 B, and Videos 5–9). Thus, the same domains of

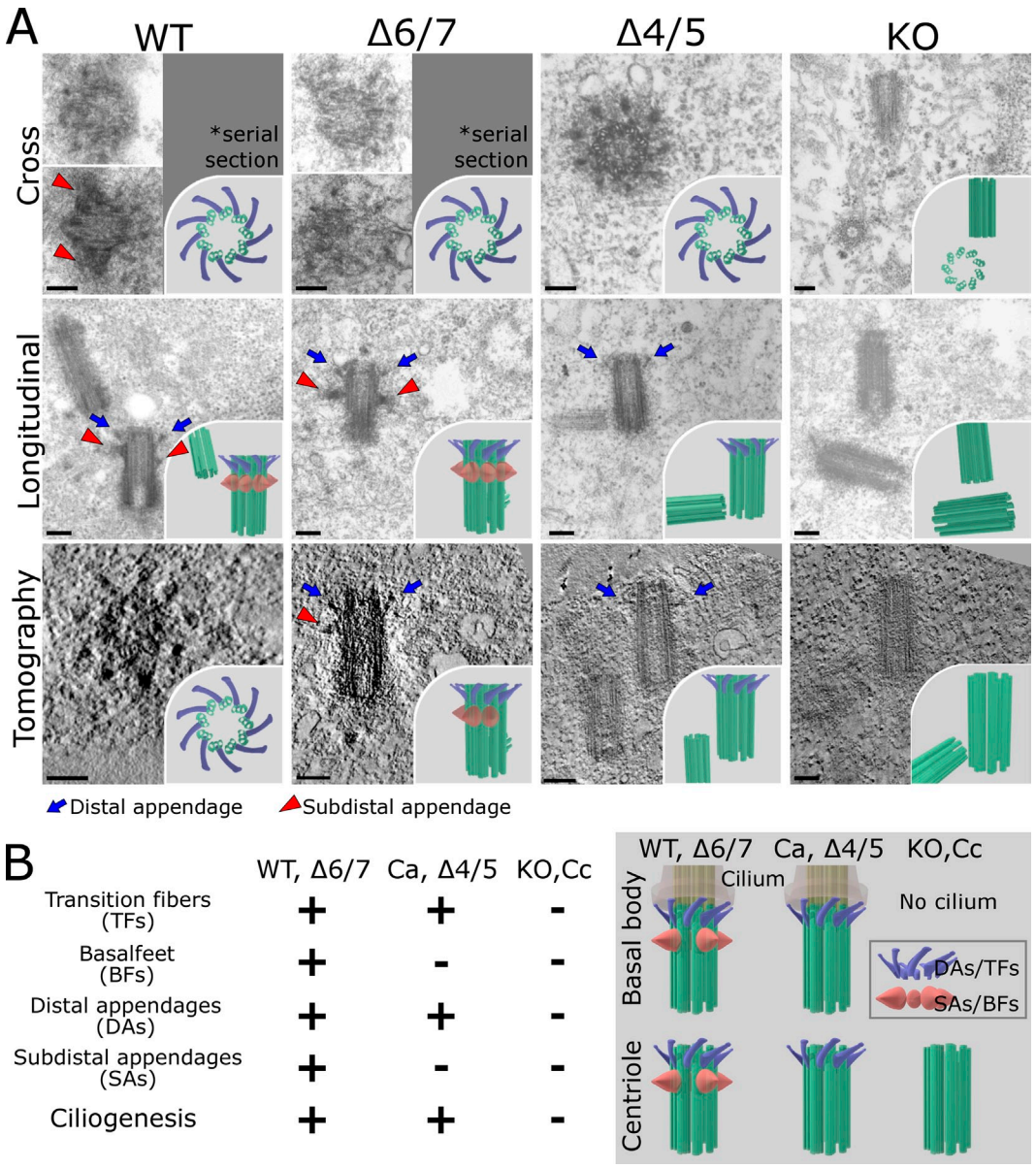

Figure 2. **Reconstitution of centriole appendages by *Odf2* deletion constructs.** (A) Electron micrographs showing distal appendages (DAs) and/or subdistal appendages (SAs) on centrioles. Thin-section electron microscopic images show cross sections (Cross) and longitudinal sections (Longitudinal) of centrioles. More than five samples were analyzed in each case. Tomography, UHVEMT images of centrioles; DAs, blue arrows; SAs, red arrowheads; WT, (DA+SA+) centriole in WT F9 cells; Δ4/5, (DA+SA−) centriole in Δ4/5 construct–expressing *Odf2*-KO F9 cells; Δ6/7, (DA+SA+) centriole in Δ6/7 construct–expressing *Odf2*-KO F9 cells; KO, (DA−SA−) centriole; TFs, blue arrows; BF, red arrowheads. Bars, 0.2 µm. Insets, schematic drawings of electron microscopic images of centrioles. (B) Summary of findings on the reconstitution of the basal body/centriole appendages.

	WT, Δ6/7	Ca, Δ4/5	KO,Cc
Transition fibers (TFs)	+	+	-
Basalfeet (BFs)	+	-	-
Distal appendages (DAs)	+	+	-
Subdistal appendages (SAs)	+	-	-
Ciliogenesis	+	+	-

Odf2 were required to form ciliary TFs and centriole DAs, suggesting that these structures had some molecular architecture and function in common.

Next, because Ex-4/5 was required for BF to form in the basal bodies of primary cilia in *Odf2*-KO F9 cells, we examined the formation of centriole SAs by Ex-4/5–containing constructs by serial thin-section EM and UHVEM. We found that all of the Ex-4/5–containing ciliogenic constructs formed SAs in centrioles. In contrast, the ciliogenic constructs lacking the Ex-4/5 sequence did not form SAs (Fig. 2 A, Fig. 3, Fig. S3 B, and Videos 6–9). Thus, the same domains of ODF2/cenexin were needed to form the basal body BF and centriole SAs, indicating that they have common molecular bases (Fig. 2 B). Together, these results supported the idea that the appendages of basal bodies and centrioles are homologous (Azimzadeh and Marshall, 2010; Seeley and Nachury, 2010; Kunimoto et al., 2012).

Immunofluorescence analysis of the molecular components in appendages reconstituted by *Odf2*

The two sets of homologous appendages on basal bodies and centrioles appear to be molecularly distinct. Their dependence on different domains of the *Odf2* gene product could result in the distinct sets of associated molecules incorporated into the different appendage types. The three patterns of reconstitution (i.e., centrioles bearing no appendages, only DAs, or DAs and

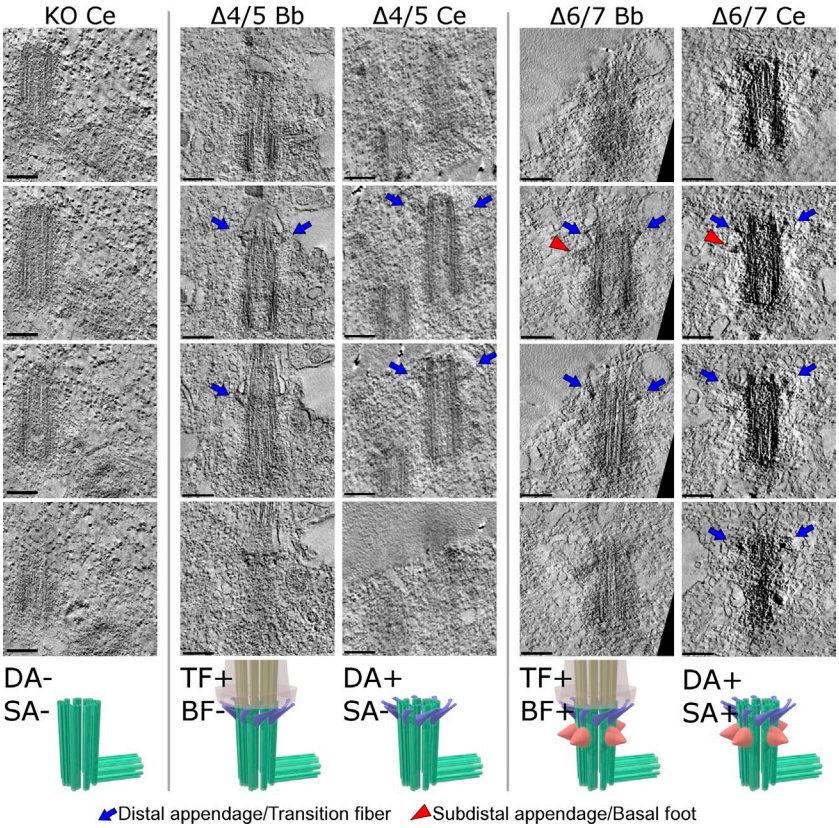

Figure 3. **Ultra-high voltage electron microscopic tomographic (UHVEMT) images of basal bodies/centrioles.** Four slices are shown (see Videos 1–9). Bb, basal body; Ce, centriole; Δ4/5 and Δ6/7, deletion mutants of *Odf2* that were exogenously expressed in *Odf2*-KO F9 cells; TFs/DAs, blue arrows; BF/SAs, red arrowheads. Bars, 0.2 µm.

SAs, depending on the sequences contained in the *Odf2* deletion construct) provided a powerful tool for confirming which molecular components are associated with DAs or SAs, respectively. We therefore examined the immunofluorescence signals for DA- and SA-associated proteins (ninein, centriolin, and CEP164) and centriole proteins (chibby and OFD1) in their respective reconstituted appendages. To examine the relative spatial relationships of the appendages in centrosomes, we stained the centrosomes with anti-GFP to visualize GFP-tagged ODF2/cenexin and with anti–γ-tubulin to label centrosomes (Fig. 4).

We first found that the distal ends of the *Odf2*-KO centrioles were negative for all the antigens except OFD1. The ninein and centriolin signals were detected at the proximal ends of mother and daughter centrioles regardless of *Odf2* expression, as previously reported (Mogensen et al., 2000; Ishikawa et al., 2005). Next, we found that centrioles associated with DAs and SAs (due to exogenous transfection of the full-length or Δ6/7 *Odf2* constructs) were positive for CEP164, ninein, centriolin, chibby, and OFD1 at their distal ends. These results strongly suggested that the DA and SA structures represent supramolecular complexes that require *Odf2* expression to form.

We then examined the appendage proteins in DA+SA− centrioles by immunofluorescence, using the Δ4/5 *Odf2* construct in *Odf2*-KO cells. We found that CEP164, a DA component, was restored on the distal end of centrioles. Chibby, an appendage component that had not been assigned to a particular appendage (Voronina et al., 2009; Steere et al., 2012), was also restored on the distal end of centrioles, although it remains to be studied whether chibby is a DA component and/or a component associated with the ciliary vesicle or transition zone, the assembly of which depends on DA-mediated membrane docking.

Centriolin was also observed at the distal end of (DA+SA−) centrioles in Δ4/5 *Odf2*-expressing *Odf2*-KO cells. This finding was unexpected because centriolin is reportedly an SA component (Gromley et al., 2003), and our data suggest that ninein and centriolin are differentially associated with SAs and that centriolin is associated with the product of the Δ4/5 *Odf2* construct (Fig. 4 B). Centriolin is reported to interact with Rab11 GTPase and to regulate its activity through Evi5 in vesicular trafficking (Gromley et al., 2005; Hehnly et al., 2012). Thus, it is most likely that centriolin, as a complex with the product of the Δ4/5 *Odf2* construct, forms the platform for Rab11-related vesicular trafficking, possibly in a different way from the case in (DA+SA+) centrioles.

Centrosomal subdistal appendages help stabilize the centrosomal microtubules

We next examined the stabilization of centrosomal microtubules in transfected cells treated with nocodazole, which interferes with microtubule polymerization. We found that under nocodazole treatment, the number of microtubules associated with centrosomes was significantly greater in wild-type (DA+SA+) cells than in *Odf2*-KO (DA−SA−) cells, based on the number of microtubules in the asters surrounding the centrioles (Fig. 5, A and B). In a previous study, we showed that the cell cycle and centrosomal microtubule-organizing center (MTOC) activity are unaffected by the loss of both appendages (Ishikawa et al., 2005). Consistent with this finding, our results of a microtubule

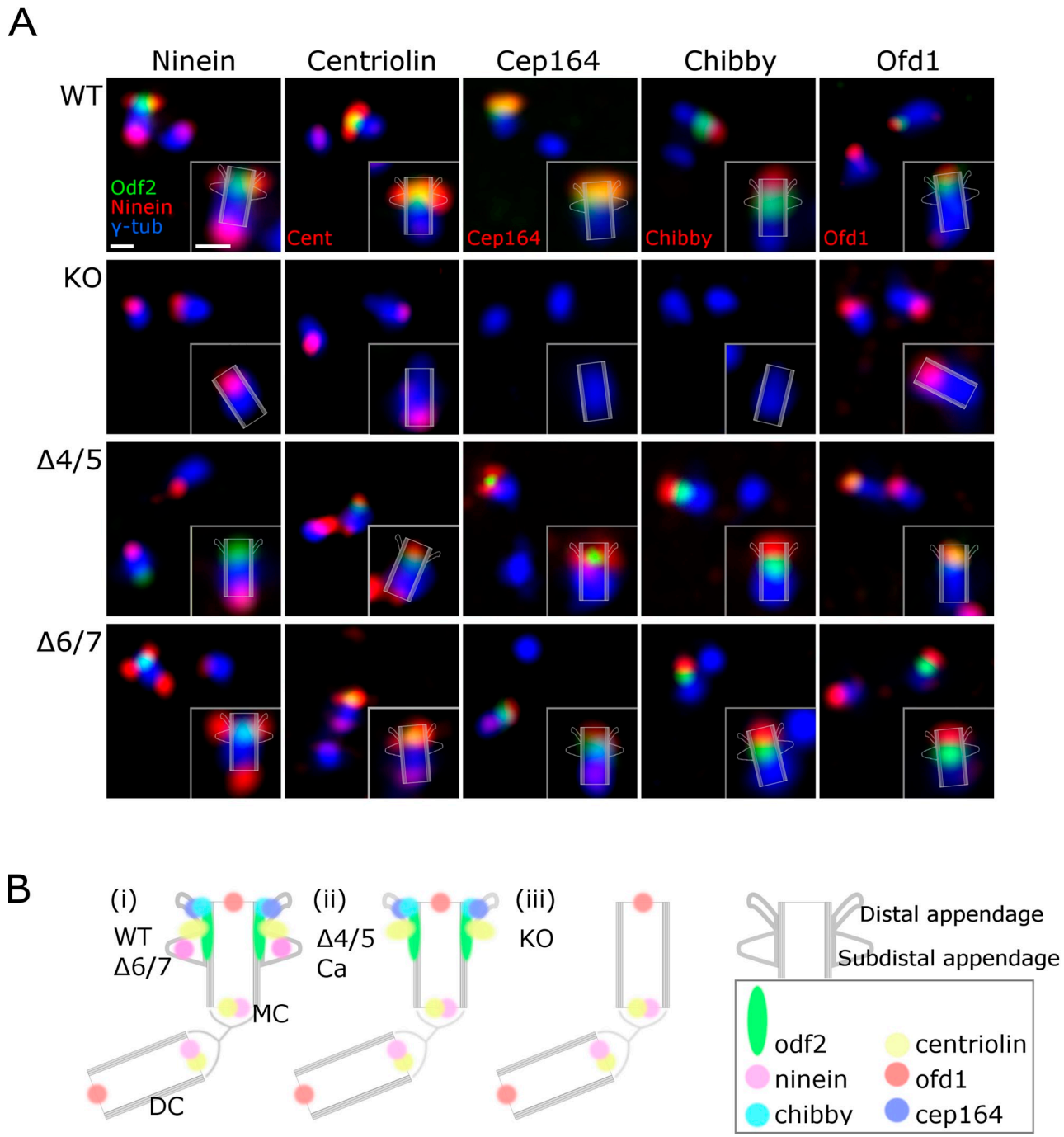

Figure 4. **Immunofluorescence microscopic images of centriole appendages in the DA+SA+, DA-SA−, and DA+SA− patterns.** (A) Immunofluorescence for ninein, centriolin, CEP164, and OFD1. WT, (DA+SA+) centriole in WT F9 cells; KO, (DA-SA−) centriole in *Odf2*-KO F9 cells; Δ4/5, (DA+SA−) centriole in Δ4/5 construct–expressing *Odf2*-KO F9 cells; Δ6/7, (DA+SA+) centriole in Δ6/7 construct–expressing *Odf2*-KO F9 cells. (B) Schematic drawing showing the localization of centrosomal components. MC, mother centriole; DC, daughter centriole. Bars, 500 nm.

regrowth assay (Brandt and Lee, 1993; Gaglio et al., 1996; Ishikawa et al., 2005) using centrosomes depleted of microtubules by prolonged nocodazole/cold treatment showed that the MTOC activity in the wild-type and *Odf2*-KO cells was the same (Fig. S3, C and D).

Similar differences were detected between SA− centrioles and those with reconstituted SAs. The number of centrosomal microtubules was not significantly higher on the DA+SA− centrioles in cells transfected with the Δ4/5 or Ca construct, compared with *Odf2*-KO (DA−SA−) cells, suggesting that the resistance to nocodazole was not increased by the presence of DAs. In contrast, the full-length or Δ6/7 *Odf2* constructs, which reconstituted both the DA and SA in *Odf2*-KO cells, increased the cells' resistance to nocodazole. These findings suggested that SA stabilizes the centrosomal microtubules against depolymerization, consistent with the idea that the DA and SA centriole appendages have distinct functions. That is, DAs are required and sufficient for ciliogenesis, whereas SAs stabilize the centrosomal microtubules.

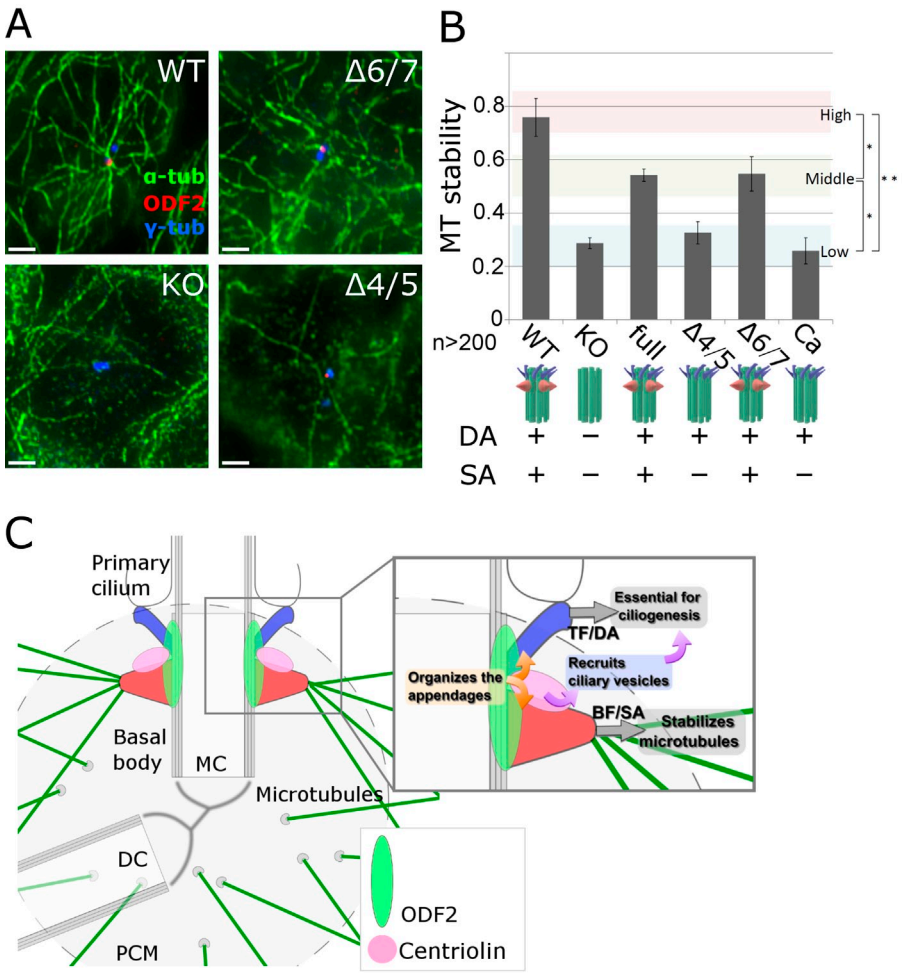

Figure 5. **Specific role of centrosomal subdistal appendages (SAs) in stabilizing centriole microtubules (MTs).** (A) Immunofluorescence images of MTs in DA+SA+, DA+SA−, and DA−SA− centrioles under nocodazole treatment, an MT-destabilizing condition. WT, (DA+SA+) centriole in WT F9 cells; Δ4/5, (DA+SA−) centriole in Δ4/5 construct–expressing *Odf2*-KO F9 cells; Δ6/7, (DA+SA+) centriole in Δ6/7 construct–expressing *Odf2*-KO F9 cells. (B) Quantification of MT stability. The relative MT stability is shown for the indicated *Odf2* construct (*, P = 0.01; **, P = 0.005; *n* > 200 in more than three independent experiments). (C) Schematic drawing of the specific roles of the appendages of ciliary basal bodies/centrioles. In the proposed model, separate domains in Odf2 serve as the molecular platform on which the appendages are constructed. Note that centriolin associates with ODF2/cenexin at the base of the SA (or where the base would be in the absence of SAs), and recruits vesicles whose cargoes support ciliogenesis. The BF/SAs (red) stabilize MTs, whereas the TFs/DAs (blue) are essential for ciliogenesis. MC, mother centriole; DC, daughter centriole.

Conclusion

We here showed that different *Odf2* sequences were required to reconstitute the basal body appendages as TF+BF− or TF+BF+, and the same sequences were required to reconstitute, respectively, the DA and SA centriole appendages. A comparison of the structural characteristics of the three appendage patterns on basal bodies (TF+BF+, TF+BF−, and TF−BF−) and on centrioles (DA+SA+, DA+SA−, DA−SA−), respectively, showed that the TFs and BF are structurally and possibly functionally homologous to the DAs and SAs, respectively. The N-terminal domain reconstituted the BF/SA on basal bodies or centrioles only when the TF/DA was formed by the C-terminal domains of *Odf2*. Alternatively, the assembly of BF/SAs could require both the N-terminal and C-terminal domains of the ODF2 protein, whether the TFs/DAs are present or not. Thus, the location of the TF/DA and BF/SA appendages at the distal end of the nine microtubule triplets might be determined primarily by the TF/DA. Given that the distinct appendage structures both depended on the *Odf2* gene product, it is likely that they are integrated in some cooperative way into a unified sophisticated system (Fig. 5 C).

In this respect, the functional relationship between the two appendage types is not simple because the SA component centriolin was found, unexpectedly, associated with SA− centrioles. Although centriolin may not be directly involved in SA formation, it may be involved in some function of the SA. In this respect, regulators of Rab8 and Rab11, such as Rabin8 and Evi5, were recently implicated in the SA/BF and DA/TF systems through centriolin and CEP164, respectively (Knödler et al., 2010; Westlake et al., 2011; Hehnly et al., 2012). Thus, ciliogenesis may represent the actions of functionally integrated systems of the TF/DA and BF/SA.

Here we showed that the distinct molecular constitutions of the appendages, which are located close to one another near the distal end of basal bodies and centrioles, are based on different *Odf2* domain usage. The transfection experiments used here provided a good tool for dissecting the molecular components of the different appendages. Furthermore, defining the different *Odf2* domains used in the formation of each appendage type provided a helpful tool for identifying new components required for building the separate appendage structures. Further studies along these lines will illuminate the molecular composition and functions of these homologous structures: the basal body–associated TFs and BF and the centriole-associated DAs and SAs. Another important future goal is to elucidate how the functional platforms associated with distinct appendages are integrated into centrosome/basal body– and microtubule-related cellular events.

Materials and methods

Antibodies

Rabbit anti-CEP164 polyclonal antibodies (pAbs) were a gift from G. Pereira (DKFZ-ZMBH Alliance, German Cancer Research Center, Heidelberg, Germany). The rat anti-ODF2 monoclonal antibody (mAb) was newly generated in our laboratory. Synthetic peptides corresponding to the C-terminal ODF2/cenexin protein sequence were used to immunize rats, and hybridoma cells were cloned by a standard method, as described previously (Tsukita et al., 1994). In short, hybridoma cells were generated by fusing immunized rat lymphocytes and P3 mouse myeloma cells. We obtained two clones, MAT159 and MAT195, named after the people who generated them (Murakami/Aihara/Tateishi). The specificities of these antibodies were examined using *Odf2*-KO F9 cells by immunofluorescence. The rat anti-centriolin mAb and rabbit anti-ninein pAb were also generated previously (Ishikawa et al., 2005). The cDNAs encoding amino acids 953–1228 of mouse ninein and 1–261 of mouse centriolin (N-centriolin) were subcloned into pGEX-4T-1 (GE Healthcare), and their GST fusion proteins were expressed in *Escherichia coli*. They were purified on glutathione Sepharose 4B columns (GE Healthcare), and used as antigens in rabbits or rats. In addition, two other anti-centriolin antibodies were used, and yielded the same results: rat anti-centriolin mAb that we generated but have not described previously, and commercially available rabbit anti-centriolin pAb (Sigma-Aldrich). The following antibodies were purchased: rabbit anti-ODF2 pAb (Abcam), rabbit anti-chibby pAb (EMD Millipore), mouse anti–α-tubulin mAb (Sigma-Aldrich), rat anti–α-tubulin mAb (Abcam), rabbit anti–γ-tubulin pAb (Sigma-Aldrich), mouse anti–γ-tubulin mAb (Sigma-Aldrich), and mouse anti-acetylated α-tubulin mAb (Sigma-Aldrich). All primary antibodies were used at a dilution of 100× to ∼1,000×. Alexa Fluor 488–, 568–, and 647–labeled secondary antibodies were commercially obtained (Invitrogen). All secondary antibodies were used at a dilution of 1,000×.

Constructs and cell culture

The product of *Odf2* (ENSMUST00000113757) was considered to be full length. The *Odf2* deletion constructs were subcloned into the pCAGGS expression vector, which is designed to express N-terminally tagged EGFP-fused proteins. F9 cells are derived from mouse embryonic teratocarcinoma, and were cultured on gelatin-coated dishes in DMEM with 10% FBS. To establish stable F9 cell lines expressing each *Odf2* construct, each expression vector was transfected into *Odf2*-KO F9 cells, which were described previously (Ishikawa et al., 2005). In F9 cells, exons 6–9 were deleted in the 22 exons of Odf2.

Microtubule stability assay

Confluent cells were transfected, cultured on coverslips, and treated with 500 nM nocodazole for 5 min at 4°C. The cells were then fixed and processed for immunofluorescence microscopy. Microtubule stability was defined as the proportion of cells showing an aster-like microtubule arrangement.

Microtubule regrowth assay

Confluent stably transfected cells were cultured on coverslips, and treated with 10 µM nocodazole for 1 h at 4°C. The cells were then washed with DMEM and incubated for another 25 min to allow microtubule regrowth (Tanaka et al., 2012). The cells were then fixed and processed for immunofluorescence microscopy.

Electron microscopy

All samples were prepared using a classical method (Ishikawa et al., 1969). F9 cells were cultured in a 6-well plate. After reaching confluence, the cells were incubated in IEM buffer (30 mM Hepes, pH 7.3, 1 mM EGTA, 0.1 mM EDTA, 25 mM NaCl, 5 mM $MgSO_4$, 1 mM DTT, and 1% volume of protease inhibitor mixture [Sigma-Aldrich]) at 37°C for 3 min. After three washes in MT-stabilizing buffer with 1 mM taxol, the cells were fixed in 2.5% glutaraldehyde, 2% formaldehyde, and 0.1% tannic acid in 100 mM Hepes buffer (pH 7.5), followed by post-fixation with 1% OsO4 in 100 mM Hepes buffer (pH 7.5). The samples were dehydrated and embedded in Epon 812 (Polysciences).

For the TEM analysis, samples were serially thin-sectioned at 50 or 70 nm, and then 15–30 serial sections were analyzed by TEM (JEM-1010; JEOL). For the ultra-high acceleration voltage electron microscopy (UHVEM) analysis, the samples were thick-sectioned at 700 nm and mounted on formvar-coated 50/75-mesh molybdenum grids. Colloidal gold particles (20-nm diameter) were deposited on both sides of each section, and the samples were observed by UHVEM at 1 or 2 MeV acceleration voltage (H-3000; Hitachi). UHVEM images were taken at 25,000×, from −60 to +60 degrees at 2-degree intervals around a single tilt axis, and images were acquired with an SSCCD camera (model F415S; TVIPS GmbH). Image calibration and 3D reconstructions of each series were performed using IMOD software (Kremer et al., 1996; The Boulder Laboratory For 3-D Electron Microscopy of Cells, Boulder, CO).

Immunofluorescence

Cells were cultured on gelatin-coated coverslips. To observe the primary cilia, the cells were incubated at 4°C for 30 min before fixation to decrease the amount of cytoplasmic acetylated microtubules. In other cases, this step was skipped. The cells were fixed in ice-cold methanol for 10 min, washed with PBS three times, and permeabilized with 0.5% Triton X-100 in PBS for 15 min. After being washed with PBS, the cells were soaked in 1% BSA in PBS for 30 min at room temperature. The cells were then incubated with primary antibodies for 1 h in a humidified chamber. The cells were then washed with PBS and incubated with Alexa Fluor 488–, 555–, or 647–conjugated secondary antibodies (Molecular Probes) for 30 min. The samples were then washed with PBS, and mounted in fluorescence mounting medium (Dako). Images were obtained with a DeltaVision system (Applied Precision) equipped with a microscope (model IX70; Olympus) and observed using 40× Plan Apo NA 1.4 and 63× Plan Apo NA 1.4 oil immersion objectives. Images of cytoplasmic microtubules were obtained using an ELYRA S.1 (SR-SIM) system (Carl Zeiss) and a 100× α-Plan Apo NA 1.46 oil immersion objective. To quantify cilia, cells displaying primary cilia were identified by immunofluorescence with an anti-acetylated α-tubulin mAb. All images were acquired at 25°C. Images were prepared using Adobe Photoshop, Illustrator (Adobe systems), and ImageJ (National Institutes of Health).

Online supplemental material

Fig. S1 provides data on the electron micrographs of appendages reconstituted on centrioles and basal bodies by the transfected Ca construct. Fig. S2 shows Western blotting analysis of *Odf2*-KO F9 cells in which GFP-tagged *Odf2* deletion constructs, used in this study, were expressed. Fig. S3 shows the serial cross sections of basal bodies and centrioles with two or one appendages, reconstituted by expression of deleted series of *Odf2*, or with no appendages. Also in Fig. S3, MTOC activity on the centrioles in wild-type and *Odf2*-KO F9 cells is shown. Video 1 shows the UHVEM tomographic images of the ciliary basal body of an *Odf2*-WT F9 cell and its schematic drawing. Video 2 shows the UHVEM tomographic images of the ciliary basal body of an *Odf2*-KO F9 cell expressing the Δ4/5 construct and its schematic drawing. Video 3 shows the UHVEM tomographic images of the ciliary basal body of an *Odf2*-KO F9 cell expressing the Δ6/7 construct and its schematic drawing. Video 4 shows the UHVEM tomographic images of the ciliary basal body of an *Odf2*-KO F9 cell expressing the Ca construct and its schematic drawing. Video 5 shows the UHVEM tomographic images of a centriole in an *Odf2*-WT F9 cell and its schematic drawing. Video 6 shows the UHVEM tomographic images of a centriole in an *Odf2*-KO cell and its schematic drawing. Video 7 shows the UHVEM tomographic images of a centriole in an *Odf2*-KO F9 cell expressing the Δ4/5 construct and its schematic drawing. Video 8 shows the UHVEM tomographic images of a centriole in an *Odf2*-KO F9 cell expressing the Δ6/7 construct and its schematic drawing. Video 9 shows the UHVEM tomographic images of a centriole in an *Odf2*-KO F9 cell expressing the Ca construct and its schematic drawing. Online supplemental material is available at http://www.jcb.org/cgi/content/full/jcb.201303071/DC1. Additional data are available in the JCB DataViewer at http://dx.doi.org/10.1083/jcb.201303071.dv.

The authors thank M. Uji, A. Hagiwara-Yano, and F. Takenaga for technical assistance, and members of our laboratories for discussion. We also thank the undergraduate students, H. Murakami and C. Aihara, for their collaboration in generating the rat anti-ODF2/cenexin mAbs (MAT159 and MAT195); and M. Sudol, as well as G. Gray and L. Miglietta, for reading our manuscript. The anti-CEP164 pAb was a gift from G. Pereira.

This work was supported in part by a Grant-in-Aid for Scientific Research on Innovative Areas and for Scientific Research (A) to S. Tsukita and by the "Nanotechnology Platform" project (no. 12024046) of the Ministry of Education, Culture, Sports, Science and Technology (MEXT), Japan.

Submitted: 13 March 2013
Accepted: 30 September 2013

References

Anderson, R.G. 1972. The three-dimensional structure of the basal body from the rhesus monkey oviduct. *J. Cell Biol.* 54:246–265. http://dx.doi.org/10.1083/jcb.54.2.246

Azimzadeh, J., and W.F. Marshall. 2010. Building the centriole. *Curr. Biol.* 20:R816–R825. http://dx.doi.org/10.1016/j.cub.2010.08.010

Bornens, M. 2002. Centrosome composition and microtubule anchoring mechanisms. *Curr. Opin. Cell Biol.* 14:25–34. http://dx.doi.org/10.1016/S0955-0674(01)00290-3

Bornens, M., M. Paintrand, J. Berges, M.C. Marty, and E. Karsenti. 1987. Structural and chemical characterization of isolated centrosomes. *Cell Motil. Cytoskeleton*. 8:238–249. http://dx.doi.org/10.1002/cm.970080305

Bouckson-Castaing, V., M. Moudjou, D.J. Ferguson, S. Mucklow, Y. Belkaid, G. Milon, and P.R. Crocker. 1996. Molecular characterisation of ninein, a new coiled-coil protein of the centrosome. *J. Cell Sci.* 109:179–190.

Brandt, R., and G. Lee. 1993. Functional organization of microtubule-associated protein tau. Identification of regions which affect microtubule growth, nucleation, and bundle formation in vitro. *J. Biol. Chem.* 268:3414–3419.

Brohmann, H., S. Pinnecke, and S. Hoyer-Fender. 1997. Identification and characterization of new cDNAs encoding outer dense fiber proteins of rat sperm. *J. Biol. Chem.* 272:10327–10332. http://dx.doi.org/10.1074/jbc.272.15.10327

Chang, P., T.H. Giddings Jr., M. Winey, and T. Stearns. 2003. Epsilon-tubulin is required for centriole duplication and microtubule organization. *Nat. Cell Biol.* 5:71–76. http://dx.doi.org/10.1038/ncb900

Dawe, H.R., H. Farr, and K. Gull. 2007. Centriole/basal body morphogenesis and migration during ciliogenesis in animal cells. *J. Cell Sci.* 120:7–15. http://dx.doi.org/10.1242/jcs.03305

Dirksen, E.R., and P. Satir. 1972. Ciliary activity in the mouse oviduct as studied by transmission and scanning electron microscopy. *Tissue Cell*. 4:389–403. http://dx.doi.org/10.1016/S0040-8166(72)80017-X

Gaglio, T., A. Saredi, J.B. Bingham, M.J. Hasbani, S.R. Gill, T.A. Schroer, and D.A. Compton. 1996. Opposing motor activities are required for the organization of the mammalian mitotic spindle pole. *J. Cell Biol.* 135:399–414. http://dx.doi.org/10.1083/jcb.135.2.399

Gibbons, I.R. 1961. The relationship between the fine structure and direction of beat in gill cilia of a lamellibranch mollusc. *J. Biophys. Biochem. Cytol.* 11:179–205. http://dx.doi.org/10.1083/jcb.11.1.179

Graser, S., Y.-D. Stierhof, S.B. Lavoie, O.S. Gassner, S. Lamla, M. Le Clech, and E.A. Nigg. 2007. Cep164, a novel centriole appendage protein required for primary cilium formation. *J. Cell Biol.* 179:321–330. http://dx.doi.org/10.1083/jcb.200707181

Gromley, A., A. Jurczyk, J. Sillibourne, E. Halilovic, M. Mogensen, I. Groisman, M. Blomberg, and S. Doxsey. 2003. A novel human protein of the maternal centriole is required for the final stages of cytokinesis and entry into S phase. *J. Cell Biol.* 161:535–545. http://dx.doi.org/10.1083/jcb.200301105

Gromley, A., C. Yeaman, J. Rosa, S. Redick, C.-T. Chen, S. Mirabelle, M. Guha, J. Sillibourne, and S.J. Doxsey. 2005. Centriolin anchoring of exocyst and SNARE complexes at the midbody is required for secretory-vesicle-mediated abscission. *Cell*. 123:75–87. http://dx.doi.org/10.1016/j.cell.2005.07.027

Guarguaglini, G., P.I. Duncan, Y.D. Stierhof, T. Holmström, S. Duensing, and E.A. Nigg. 2005. The forkhead-associated domain protein Cep170 interacts with Polo-like kinase 1 and serves as a marker for mature centrioles. *Mol. Biol. Cell*. 16:1095–1107. http://dx.doi.org/10.1091/mbc.E04-10-0939

Hehnly, H., C.T. Chen, C.M. Powers, H.L. Liu, and S. Doxsey. 2012. The centrosome regulates the Rab11- dependent recycling endosome pathway at appendages of the mother centriole. *Curr. Biol.* 22:1944–1950. http://dx.doi.org/10.1016/j.cub.2012.08.022

Hoyer-Fender, S. 2010. Centriole maturation and transformation to basal body. *Semin. Cell Dev. Biol.* 21:142–147. http://dx.doi.org/10.1016/j.semcdb.2009.07.002

Ibi, M., P. Zou, A. Inoko, T. Shiromizu, M. Matsuyama, Y. Hayashi, M. Enomoto, D. Mori, S. Hirotsune, T. Kiyono, et al. 2011. Trichoplein controls microtubule anchoring at the centrosome by binding to Odf2 and ninein. *J. Cell Sci.* 124:857–864. http://dx.doi.org/10.1242/jcs.075705

Ishikawa, H., R. Bischoff, and H. Holtzer. 1969. Formation of arrowhead complexes with heavy meromyosin in a variety of cell types. *J. Cell Biol.* 43:312–328. http://dx.doi.org/10.1083/jcb.43.2.312

Ishikawa, H., A. Kubo, S. Tsukita, and S. Tsukita. 2005. Odf2-deficient mother centrioles lack distal/subdistal appendages and the ability to generate primary cilia. *Nat. Cell Biol.* 7:517–524. http://dx.doi.org/10.1038/ncb1251

Knödler, A., S. Feng, J. Zhang, X. Zhang, A. Das, J. Peränen, and W. Guo. 2010. Coordination of Rab8 and Rab11 in primary ciliogenesis. *Proc. Natl. Acad. Sci. USA*. 107:6346–6351. http://dx.doi.org/10.1073/pnas.1002401107

Kobayashi, T., and B.D. Dynlacht. 2011. Regulating the transition from centriole to basal body. *J. Cell Biol.* 193:435–444. http://dx.doi.org/10.1083/jcb.201101005

Kremer, J.R., D.N. Mastronarde, and J.R. McIntosh. 1996. Computer visualization of three-dimensional image data using IMOD. *J. Struct. Biol.* 116:71–76. http://dx.doi.org/10.1006/jsbi.1996.0013

Kunimoto, K., Y. Yamazaki, T. Nishida, K. Shinohara, H. Ishikawa, T. Hasegawa, T. Okanoue, H. Hamada, T. Noda, A. Tamura, et al. 2012. Coordinated ciliary beating requires Odf2-mediated polarization of basal bodies via basal feet. *Cell*. 148:189–200. http://dx.doi.org/10.1016/j.cell.2011.10.052

Lange, B.M., and K. Gull. 1995. A molecular marker for centriole maturation in the mammalian cell cycle. *J. Cell Biol.* 130:919–927. http://dx.doi.org/10.1083/jcb.130.4.919

Mogensen, M.M., A. Malik, M. Piel, V. Bouckson-Castaing, and M. Bornens. 2000. Microtubule minus-end anchorage at centrosomal and non-centrosomal sites: the role of ninein. *J. Cell Sci.* 113:3013–3023.

Nakagawa, Y., Y. Yamane, T. Okanoue, S. Tsukita, and S. Tsukita. 2001. Outer dense fiber 2 is a widespread centrosome scaffold component preferentially associated with mother centrioles: its identification from isolated centrosomes. *Mol. Biol. Cell.* 12:1687–1697. http://dx.doi.org/10.1091/mbc.12.6.1687

Nigg, E.A., and T. Stearns. 2011. The centrosome cycle: Centriole biogenesis, duplication and inherent asymmetries. *Nat. Cell Biol.* 13:1154–1160. http://dx.doi.org/10.1038/ncb2345

Oko, R., and Y. Clermont. 1988. Isolation, structure and protein composition of the perforatorium of rat spermatozoa. *Biol. Reprod.* 39:673–687. http://dx.doi.org/10.1095/biolreprod39.3.673

Paintrand, M., M. Moudjou, H. Delacroix, and M. Bornens. 1992. Centrosome organization and centriole architecture: their sensitivity to divalent cations. *J. Struct. Biol.* 108:107–128. http://dx.doi.org/10.1016/1047-8477(92)90011-X

Reed, W., J. Avolio, and P. Satir. 1984. The cytoskeleton of the apical border of the lateral cells of freshwater mussel gill: structural integration of microtubule and actin filament-based organelles. *J. Cell Sci.* 68:1–33.

Ren, M., G. Xu, J. Zeng, C. De Lemos-Chiarandini, M. Adesnik, and D.D. Sabatini. 1998. Hydrolysis of GTP on rab11 is required for the direct delivery of transferrin from the pericentriolar recycling compartment to the cell surface but not from sorting endosomes. *Proc. Natl. Acad. Sci. USA*. 95:6187–6192. http://dx.doi.org/10.1073/pnas.95.11.6187

Schmidt, K.N., S. Kuhns, A. Neuner, B. Hub, H. Zentgraf, and G. Pereira. 2012. Cep164 mediates vesicular docking to the mother centriole during early steps of ciliogenesis. *J. Cell Biol.* 199:1083–1101. http://dx.doi.org/10.1083/jcb.201202126

Seeley, E.S., and M.V. Nachury. 2010. The perennial organelle: assembly and disassembly of the primary cilium. *J. Cell Sci.* 123:511–518. http://dx.doi.org/10.1242/jcs.061093

Sillibourne, J.E., C.G. Specht, I. Izeddin, I. Hurbain, P. Tran, A. Triller, X. Darzacq, M. Dahan, and M. Bornens. 2011. Assessing the localization of centrosomal proteins by PALM/STORM nanoscopy. *Cytoskeleton (Hoboken)*. 68:619–627. http://dx.doi.org/10.1002/cm.20536

Sorokin, S. 1962. Centrioles and the formation of rudimentary cilia by fibroblasts and smooth muscle cells. *J. Cell Biol.* 15:363–377. http://dx.doi.org/10.1083/jcb.15.2.363

Steere, N., V. Chae, M. Burke, F.Q. Li, K. Takemaru, and R. Kuriyama. 2012. A Wnt/beta-catenin pathway antagonist Chibby binds Cenexin at the distal end of mother centrioles and functions in primary cilia formation. *PLoS ONE*. 7:e41077. http://dx.doi.org/10.1371/journal.pone.0041077

Tanaka, N., W. Meng, S. Nagae, and M. Takeichi. 2012. Nezha/CAMSAP3 and CAMSAP2 cooperate in epithelial-specific organization of noncentrosomal microtubules. *Proc. Natl. Acad. Sci. USA*. 109:20029–20034. http://dx.doi.org/10.1073/pnas.1218017109

Tanos, B.E., H.J. Yang, R. Soni, W.J. Wang, F.P. Macaluso, J.M. Asara, and M.F.B. Tsou. 2013. Centriole distal appendages promote membrane docking, leading to cilia initiation. *Genes Dev.* 27:163–168. http://dx.doi.org/10.1101/gad.207043.112

Tsukita, S., K. Oishi, N. Sato, J. Sagara, A. Kawai, and S. Tsukita. 1994. ERM family members as molecular linkers between the cell surface glycoprotein CD44 and actin-based cytoskeletons. *J. Cell Biol.* 126:391–401. http://dx.doi.org/10.1083/jcb.126.2.391

Ullrich, O., S. Reinsch, S. Urbé, M. Zerial, and R.G. Parton. 1996. Rab11 regulates recycling through the pericentriolar recycling endosome. *J. Cell Biol.* 135:913–924. http://dx.doi.org/10.1083/jcb.135.4.913

Vladar, E.K., and T. Stearns. 2007. Molecular characterization of centriole assembly in ciliated epithelial cells. *J. Cell Biol.* 178:31–42. http://dx.doi.org/10.1083/jcb.200703064

Vorobjev, I.A., and Y.S. Chentsov. 1982. Centrioles in the cell cycle. I. Epithelial cells. *J. Cell Biol.* 93:938–949. http://dx.doi.org/10.1083/jcb.93.3.938

Voronina, V.A., K. Takemaru, P. Treuting, D. Love, B.R. Grubb, A.M. Hajjar, A. Adams, F.Q. Li, and R.T. Moon. 2009. Inactivation of Chibby affects function of motile airway cilia. *J. Cell Biol.* 185:225–233. http://dx.doi.org/10.1083/jcb.200809144

Westlake, C.J., L.M. Baye, M.V. Nachury, K.J. Wright, K.E. Ervin, L. Phu, C. Chalouni, J.S. Beck, D.S. Kirkpatrick, D.C. Slusarski, et al. 2011. Primary cilia membrane assembly is initiated by Rab11 and transport protein particle II (TRAPPII) complex-dependent trafficking of Rabin8 to the centrosome. *Proc. Natl. Acad. Sci. USA*. 108:2759–2764. http://dx.doi.org/10.1073/pnas.1018823108